Biosensors and Bioelectronics 32 (2012) 244–249

Contents lists available at SciVerse ScienceDirect

Biosensors and Bioelectronics

journal homepage: www.elsevier.com/locate/bios

A hairpin DNA aptamer coupled with groove binders as a smart switch for a field-effect transistor biosensor

Tatsuro Goda, Yuji Miyahara*

Institute of Biomaterials and Bioengineering, Tokyo Medical and Dental University (TMDU), 2-3-10 Kanda-Surugadai, Chiyoda, Tokyo 101-0062, Japan

ARTICLE INFO

Article history:
Received 11 October 2011
Received in revised form
28 November 2011
Accepted 14 December 2011
Available online 24 December 2011

Keywords:
Field-effect transistor
Groove binder
Hairpin aptamer
Molecular switch
Thermo-responsiveness
Self-assembled monolayer

ABSTRACT

We report here that a hairpin-structured DNA that possesses an anti-ATP aptamer sequence successfully detected target ATP or adenosine in a temperature-dependent manner by nanoscale intramolecular displacement on the surface of a gold electrode as an extended gate of a field-effect transistor (FET). The structural switching of the hairpin aptamer from closed loop to open-loop conformations was accompanied by the release of the preloaded DNA binder (DAPI) from the stem part of the hairpin aptamer into the solution phase. The loss of intrinsic positive charges of DAPI (2+) from the diffusion layer at the gate/solution nano-interface as a result of target capturing was responsible for generating a specific signal by the field-effect. We emphasize a new aspect of the structured DNA aptamer in combination with FET: the DAPI-loaded hairpin aptamer successfully detected even uncharged adenosine, which remains a major challenge for FET-based biosensors. Given the simplicity in design of the primary and secondary structures of oligonucleotide aptamers, it is easy to apply this technology to a wide variety of bio-analytes, irrespective of their electric charges. In view of these advantages, our findings may offer a new trend in the design of stimuli-responsive "smart" biomolecular switches for semiconductor-based biosensors.

1. Introduction

Field-effect transistor (FET)-based biosensors are of great interest because of their versatility in label-free sensing of nucleic acids, proteins, viruses, and cells (Bergveld, 1986; Fritz et al., 2002; Fromherz et al., 1991; Lee et al., 2009; Poghossian et al., 2005; Sakata and Miyahara, 2008; Souteyrand et al., 1997). A combination of biochemistry, electrochemistry, solid-state physics and surface physics, together with knowledge of bioengineering, is a requisite for producing such artificial functional hybrid systems. A sensitive and specific recognition of target analytes at the solid/liquid interface corresponds to a high-affinity ligand molecule immobilized on the gate surface. Recently, nucleic acid-based aptamers have been recognized as an alternative receptor to antibodies in analytical science because of their strong affinity (nanomolar level in K_d) and excellent specificity for target molecules, as well as their advanced features such as chemical and thermal stability, equal quality, small size, and ease of modification (Bock et al., 1992; Jayasena, 1999; Wilson and Szostak, 1999). In particular, structured nucleotide aptamers can induce large signals by changing their conformation upon target recognition in the presence of a reporter molecule, allowing highly sensitive and specific detection (Famulok et al., 2007; Liu et al., 2009; Nutiu and Li, 2003; Piatek et al., 1998; Privett et al., 2010; Tang et al., 2008; Tyagi et al., 1998; Tyagi and Kramer, 1996). A large conformational change of DNA has been successfully identified by electrochemical impedance techniques (Bonanni et al., 2006; Bonanni and Pumera, 2011; Goda and Miyahara, 2011; Gong et al., 2009; Liu et al., 2011). Generally, FET devices are expected for their use in biosensing by directly transforming the intrinsic charges of target analytes into a potentiometric signal via the field effect; the electrostatic interactions between charged analytes or ions trapped on the gate surface and the electrons located at the inversion layer of the source–drain channel in the transistor can induce an electronic signal. On the other hand, this proof-of-concept determines the fate of bio-transistors that induce no overt signal upon recognition of electrically neutral species. In addition, the common issues faced by conventional FETs derive from the effect of charge-screening by dissolved mobile counterions in a buffer solution on a sensor response (Stern et al., 2007). The electric charge of solution-based biomolecules is screened at a certain length scale termed the Debye screening length. The Debye length is described as a function of ionic strength of the solution ($\propto I^{-1/2}$) and yields no more than 10 nm even in a diluted buffer solution of 1 mM. Consequently, the FET biosensor is able to distinguish the intrinsic charges of analytes located within the range of the Debye length from the gate surface in a buffer solution (Goda and Miyahara, 2010a; Kajiyama et al., 2003; Stern et al., 2007). We have been trying to organize systems that allow the Debye length-free detections to expand the utility of the FET biosensor for detecting a wide

* Corresponding author. Tel.: +81 3 5280 8095; fax: +81 3 5280 8095.
E-mail address: miyahara.bsr@tmd.ac.jp (Y. Miyahara).

0956-5663/$ – see front matter © 2011 Elsevier B.V. All rights reserved.
doi:10.1016/j.bios.2011.12.022

variety of target species, even for neutral analytes. Recently, we have achieved this challenge by making use of a stimuli-responsive polymer gel that transduces the recognition events of uncharged glucose into a dramatic permittivity change synchronized with the volume phase transition of the gel (Matsumoto et al., 2009).

In this study, we report that a hairpin-structured aptamer with a stem-loop configuration containing an adenosine 5′-triphosphate (ATP)-binding sequence cues electrical signals when its conformation changes from closed loop to open-loop upon target recognition in a label-free manner using the FET biosensor in combination with a groove binder for DNA duplex. The FET biosensor directly detects local changes in ion concentration at the gate-solution interface by the release of a positively charged DNA binder, 4′,6-diamidino-2-phenylindole (DAPI), from the stem of the hairpin aptamer upon target-induced denaturation. The structured oligonucleotide aptamer directly functions as a molecular switch at the gate/solution interface. The release of the cationic DNA binder from the aptamer DNA probe overcomes the underlying limitations of FET biosensors, allowing detection of electrically neutral target species and the Debye length-free monitoring.

2. Experimental

Synthetic oligo-DNA probes were purchased from Tsukuba Oligo Service (Tsukuba, Ibaraki, Japan). ATP, GTP, adenosine, guanosine, and DAPI were purchased from Sigma–Aldrich Japan (Tokyo, Japan) and were used without further purification. A smooth sputtered gold electrode (100 nm in thickness and 1.8 nm in RMS roughness) was cleaned before use with piranha solution (H_2O_2/H_2SO_4 = 30/70 vol/vol). (Extreme caution must be exercised when using piranha etch. An explosion-proof hood should be used.) Mixed SAMs of the hairpin aptamers and MCH were prepared on the gold electrode by two-step chemisorption; the electrode was subjected to 1 μM aptamer in 15 mM DPBS (pH 7.4) for 16 h, followed by a 16-h deposition in 1 mM MCH in ethanol. After rinsing, the electrode was heat-denatured at 90 °C for 2 h and then slowly annealed to allow self-hybridization.

Real-time changes in the interfacial potential (no bias DC voltage vs. an Ag/AgCl reference electrode) was monitored using a home-built signal processor equipped with an FET chip in an extended gate configuration (see supplemental information). The FET-sensor platform showed negligible drift (less than 1 mV/day) under stable condition and quick response (below 10 ms). After stabilizing the gate potential in 15 mM DPBS for 2 h and preloading DAPI into the stem by incubating in the 10 μM DAPI solution for 1 h, the electrode was incubated in various concentrations of ATP solution in 15 mM DPBS for each 10 min. The ATP concentration was increased in a stepwise manner. The mean value and standard deviation were obtained from at least four independent measurements.

The melt curve of each aptamer probe was acquired with continuous fluorescence recording on the SYBR Green I (Life Technologies Japan, Tokyo, Japan) in 15 mM DPBS containing the 10-μM aptamer using a ramping rate of 1 °C min^{-1} for 10–90 °C after heat denaturing at 95 °C for 15 s followed by cooling to 10 °C for 1 min. The differentiated data were analyzed using the StepOne Software v2.1 (Life Technologies).

3. Results and discussion

3.1. Characterization of mixed SAM

DNA aptamer probes containing ATP-binding sites and a self-hybridizing region were designed as a molecular recognition element (Fig. 1). Two hairpin aptamers with different stem lengths of 14-mer (long hairpin, lh) and 7-mer (short hairpin, sh) were used.

Table 1
Probe density and total packing density of the SAM formed on the gold electrode.

SAM type	Probe density/10^{-2} nm^{-2}	Total SAM density/nm^{-2}
sh-aptamer/MCH mix	1.1 ± 0.4	4.9 ± 0.5
lh-aptamer/MCH mix	1.2 ± 0.2	4.9 ± 0.5
ln-aptamer/MCH mix	1.4 ± 0.1	4.3 ± 0.3
MCH alone	None	4.4 ± 0.7

The melting temperature (T_m) of the hairpin aptamers was tunable by controlling the stem length. The aptamer with a linear (ln) conformation served as a control to evaluate the structural switching upon ATP recognition for signal induction. The known anti-ATP aptamer sequence used possesses high affinity and specificity for target ATP, but not for its triphosphate analogues (Huizenga and Szostak, 1995). The hairpin aptamer with 5′ HS-$(CH_2)_6$– was covalently linked to the gold electrode that was extended to the gate of the FET biosensor. We conducted chronocoulometry (CC) for determining the probe density of the oligo-DNA aptamers presented in the mixed SAM on the gold electrode (see supplemental information) (Steel et al., 1998). The surface density of the series of aptamers was determined, as shown in Table 1, when the surfaces were prepared at the bulk aptamer concentration of 1 μM. The relatively low probe density allows sufficient interstitial space to form short hairpins (the DNA duplex is 2.2–2.6 nm wide) while preventing intermolecular cross-hybridization between adjacent aptamers. The rest of the gold surface was backfilled with 6-mercapto-1-hexanol (MCH) to construct a densely packed SAM for preventing the nonspecific adsorption of molecules. The total packing density of the SAM was determined by cyclic voltammetry (Yang et al., 1996). The packing density of the mixed SAMs was consistent with saturation coverage of the SAM on Au(1 1 1) (Table 1) (Poirier and Tarlov, 1994).

3.2. Signal generation by selective release of DAPI from the hairpin aptamer upon target recognition

Fig. 1 shows the working principle of the aptamer FET biosensor at the nano-interface. Positively charged DAPI molecules that are selective to the minor groove of double-stranded (ds) DNA bind to the stem of the hairpin-aptamers as an electrical reporter molecule (Banerjee and Pal, 2008; Sriram et al., 1992). When target ATP is added, the hairpin aptamer probes undergo intramolecular displacement by the formation of a stable complex of the single-stranded (ss) DNA aptamer with ATP. This nano-structural transition is accompanied by the release of DAPI from the stem to the solution phase. The significant loss of positive charges from the sh-aptamers at the gate-solution nano-interface is directly transduced into electronic signals by the field-effect (Bergveld, 1986; Fritz et al., 2002; Fromherz et al., 1991; Lee et al., 2009; Poghossian et al., 2005; Sakata and Miyahara, 2008; Souteyrand et al., 1997). In the configuration of the FET-integrated circuit for signal processing, the potentiometric variation ($\Delta\varphi$) can be simply described as:

$$\Delta\varphi = \frac{\Delta Q}{C} \quad (1)$$

where ΔQ and C denote the change in the total charge at the gate-solution nano-interface and electrical double-layer capacitance, respectively. Eq. (1) indicates the loss of positive charges at the interface yields a negative potential shift.

The gold electrode modified with the sh-aptamer/MCH SAM and the DAPI indicator responded specifically to target ATP with an observed change in potential of about −17 mV at 37 °C (Fig. 2a). In contrast, no significant signals were observed for the surface incubated with non-target guanosine 5′-triphosphate (GTP) over the investigated concentration range. Because the anti-ATP aptamer sequence has no affinity for GTP, the probe remains folded

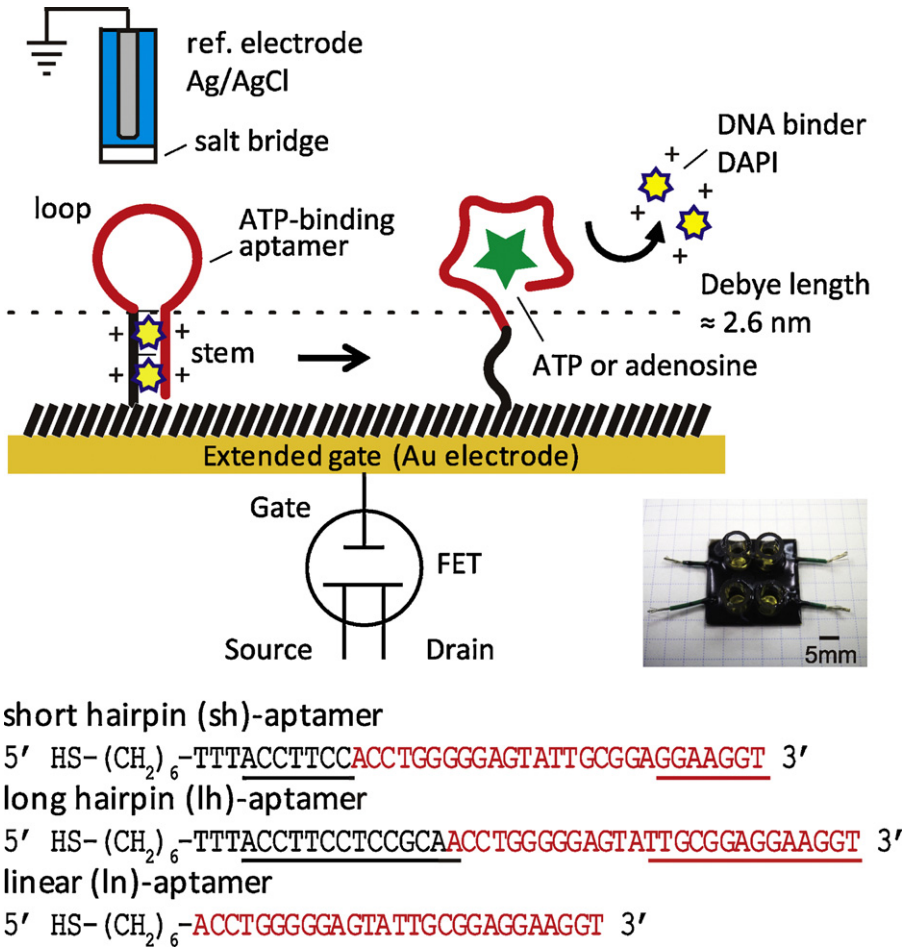

Fig. 1. Schematic representation showing signal transduction upon conformational switching of the short hairpin (sh)-aptamer accompanied by the release of the cationic DNA binder (DAPI) upon detection of ATP on the extended gate of an FET. The release of divalent DAPI from the stem of the sh-aptamer probes induced by the formation of an ATP-aptamer complex generates electrical signals by the field-effect. Picture: Au electrodes as extended gates. The sequence shown in red is the ATP-binding aptamer region and the underlined sequences from the stem. The linear (ln)-aptamer serves as a control. (For interpretation of the references to color in this figure legend, the reader is referred to the web version of this article.)

(closed-loop) and DAPI remains bound to the duplex of the stem. The observed negative change in potential following incubation with ATP is explained by the release of positively charged DAPI from the minor grooves of the A–T region of the sh-aptamer to the solution phase. Up to three molecules of DAPI may be released from each sh-aptamer (i.e., up to six positive charges) upon the target recognition event. This explanation is consistent with the unchanged electrical potential observed for the sh-aptamer-immobilized electrode used to detect ATP without including DAPI (Fig. 2b). Although the ln-aptamer has the ability to capture target ATP, the electrode covalently linked to the ln-aptamer failed to induce specific signals (Fig. 2c). Therefore, both the configuration of the short hairpin and the DAPI indicator are required to sense the presence of ATP. As shown in Fig. 2a, the response of the sensor was proportional to the concentration of ATP in the semi-logarithmic plots over a wide dynamic range (from 10^{-14} to 10^{-4} M, slope: −1.8 mV/decade). The signals between ATP and GTP were statistically significant ($p < 0.01$) at their concentrations higher than 10 nM. The sensitivity is relatively high for a simple label-free technique (yet the DAPI reporter is contained) and is comparable to most electrochemical and fluorescent measurements for ATP (Li et al., 2009; Wang and Liu, 2008; Yao et al., 2009; Zhang et al., 2010; Zhen et al., 2010). However, we notice that it is important to reduce noises and error bars to make use of this sensor for monitoring ATP concentration in real samples.

In principle, the FET biosensor can transform intrinsic charges of captured molecules, which are located inside the electrical double layer. The monitoring of the interfacial potential was performed in a dilute buffer (Dulbecco's phosphate buffered saline; DPBS, pH 7.4, 15 mM) to modulate the characteristic screening length of the solution (2.6 nm) to be comparable to the stem length of the hairpin aptamers (2.4 nm). The solution Debye length (κ^{-1}) is described as a function of ionic strength of the solution (i.e., the total number of ions) as:

$$\kappa^{-1} = \left(\frac{\varepsilon_r \varepsilon_0 k_B T}{2 N_A e^2 I}\right)^{1/2} \quad (2)$$

where $\varepsilon_r\varepsilon_0$ is the total permittivity of water, k_BT is the Boltzmann energy, N_A is Avogadro's number, e is the elementary charge, and I is the ionic strength of the solution in mol L^{-1}. Considering the intramolecular distance of a base of 0.34 nm, only the 7-mer at the 5′ end of the hairpin aptamers fits within the Debye length. Hence, the FET biosensor is sensitive and specific to variation in the charges of the stem region because of the dissociation of DAPI upon capturing ATP. In contrast, in the absence of the DAPI indicator, changes in the local ion concentration at the nano-interface caused by a large conformational switching of the hairpin aptamer are insufficient to induce potentiometric variation. We suggest that a dramatic change in the flexibility by dsDNA–ssDNA transition at the stem part may involve the failure of signal generation under the condition without DAPI incorporation. Although it appears that many negatively charged phosphates are pulled out of the Debye

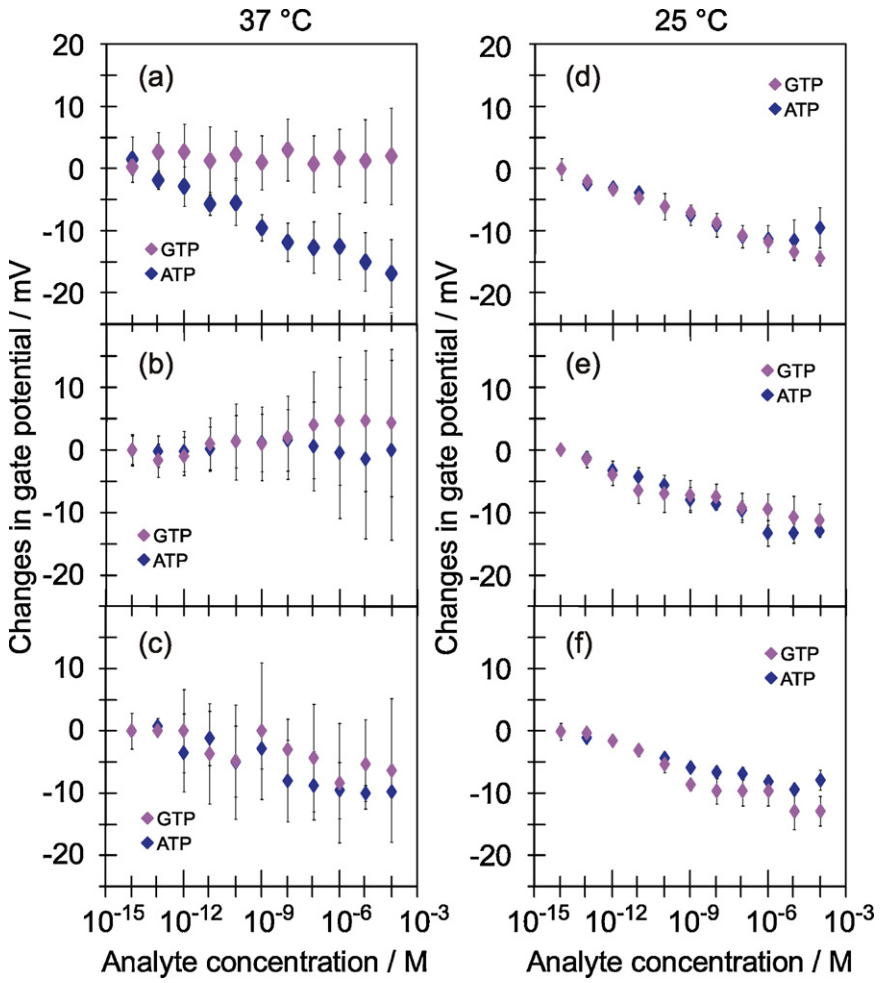

Fig. 2. Changes in the interfacial potential as a function of the logarithmic concentration of target ATP or non-target GTP measured at 37 °C (a–c) and 25 °C (d–f) using an extended-gate FET biosensor: a gold electrode bound to the sh-aptamer with DAPI (a and d), the sh-aptamer without DAPI (b and e), and the ln-aptamer with DAPI (c and f). The changes in potential were obtained in a solution of DPBS (15 mM). $n = 4$.

layer by the binding event (Fig. 1), more nucleotides are likely to come into the Debye layer due to the flexible ssDNA conformation and the total number of negative charges corresponding to the phosphates in the Debye layer do not simply decrease to a half by the binding event. Indeed, the persistence length which characterizes the flexibility of linear macromolecule decreases form 50 nm to about 2–3 nm by dsDNA–ssDNA transition in a dilute salt solution (Livolant and Leforestier, 1996; Tinland et al., 1997). In addition, the counterion-screening effect for the aptamer probe at the gate/solution interface is another reason for the insensitive detection of a structural transition in the absence of DAPI.

Interestingly enough, no significant changes in the potential were observed at 25 °C (Fig. 2d–f). The results indicate that the hairpin aptamers must be thermally activated to overcome the free energy barrier caused by the intramolecular base pairing at the state of a closed-loop hairpin configuration (Urata et al., 2007). We measured the melt-curve of the hairpin aptamers in the presence of ATP or GTP in the buffer solution (Fig. 3). The T_m that corresponds to the denaturing of the sh-aptamer was calculated in advance to be 49 °C using the mfold web calculator (http://mfold.rna.albany.edu/?q=mfold). The experimental T_m of the sh-aptamer dropped from 50 to 38 °C only in the presence of target ATP (10^{-5} M) in the buffer solution. This transition of T_m strongly corresponds to the temperature at which the sh-aptamer can induce the specific signals upon capturing ATP. There was no such transition of the T_m for the lh-aptamer and the ln-aptamer. The hairpin aptamer designed to form the longer stem (14-mer) is more thermodynamically stable ($T_m = 70$ °C) at the closed-loop conformation by intramolecular Watson-Crick base-pairing than the hairpin aptamer designed to form the aptamer-ATP complex. Additional peaks in the melt curves indicate the presence of structurally possible variants of the hairpin aptamer probes over the low temperature range of <50 °C. We infer that the monotonous drifts in the negative direction for the potentiometric signal over the analyte concentration range at 25 °C are attributed to the detection of nonspecific adsorption of the negatively charged triphosphate moiety in ATP and GTP onto the positively charged MCH-SAM on gold at the no bias potential versus the reference Ag/AgCl electrode (Rentsch et al., 2007). Furthermore, the structural transition of the sh-aptamer covalently linked to the gold electrode was identified by epifluorescent images in the presence of the fluorescent stain (TO-PRO-3) that allows ultrasensitive and specific detections of dsDNA (Van Hooijdonk et al., 1994; Goda and Miyahara, 2011). These results support the proof-of-concept of the aptamer FET biosensor that the sh-aptamer functions as a smart molecular switch upon target recognition, as shown in Fig. 1.

The results suggest that the sensing mechanism by structural displacement of the sh-aptamer followed by the release of the charged reporter molecules allows the detection of a target analyte independent of its electric charges. To support the sensing mechanism, we performed the selective detection of adenosine instead of ATP using the sh-aptamer-derivatized FET

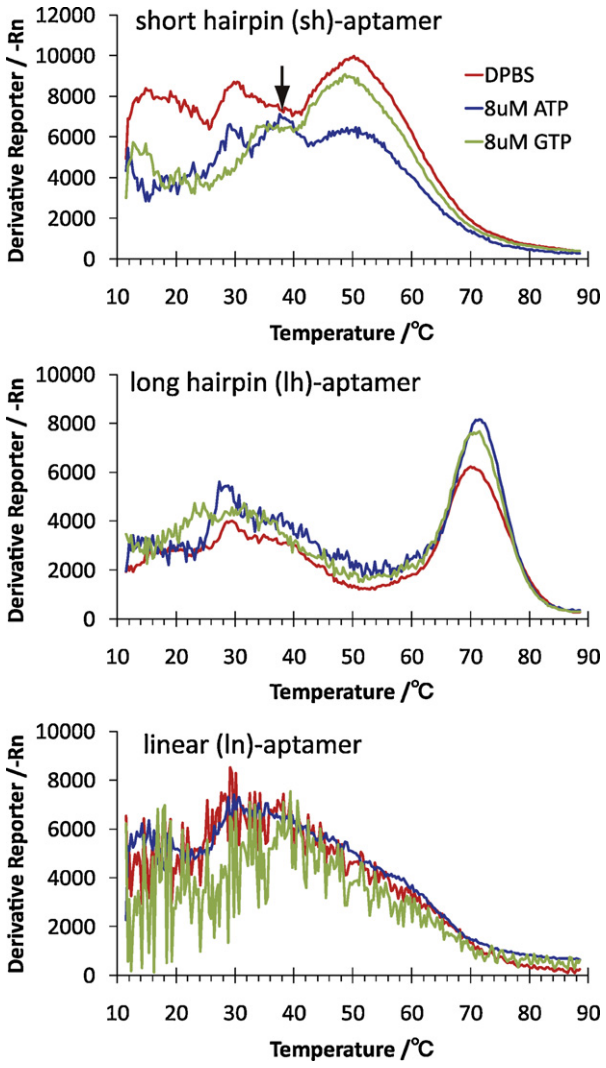

Fig. 3. Identification of the melt curves for the short hairpin (sh)-aptamer, long hairpin (lh)-aptamer, and linear (ln)-aptamer using the fluorescent intercalator (SYBR green) in 15 mM DPBS solution with 8 μM ATP or GTP. An arrow indicates the newly observed T_m for the sh-aptamer in the presence of ATP. (For interpretation of the references to color in this figure legend, the reader is referred to the web version of this article.)

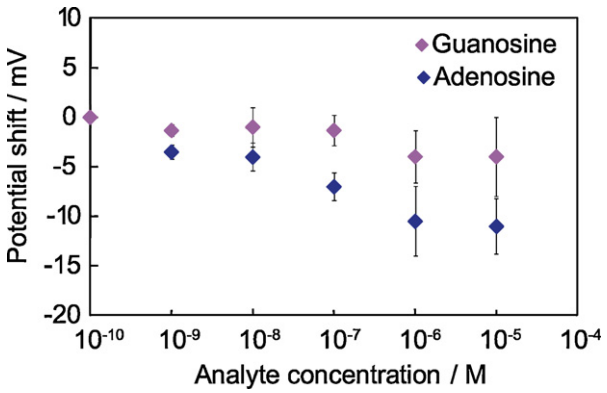

Fig. 4. Changes in the interfacial potential as a function of the concentration of target adenosine or non-target guanosine measured at 37 °C on the gold electrode bound to the sh-aptamer/MCH SAM with DAPI.

biosensor. Since the adenosine group is the epitope for the anti-ATP aptamer (Huizenga and Szostak, 1995), the sh-aptamer is also capable of capturing adenosine as well as ATP with high sensitivity and selectivity. In contrast to charge state of ATP (−4) at pH 7.4, adenosine is electrically neutral under physiological pH. Fig. 4 represents the successful detection of adenosine using the sh-aptamer-derivatized gold electrode with the DAPI indicator at 37 °C. The aptamer FET biosensor in combination with the electronic reporter molecule realizes the sensitive and selective detection of neutral adenosine at the dynamic concentration range from 10^{-8} to 10^{-6} M.

FETs are a well-known powerful transducer for detecting ions or charged species as an electronic signal in a label-free manner (Bergveld, 1986; Fritz et al., 2002; Fromherz et al., 1991; Lee et al., 2009; Poghossian et al., 2005; Sakata and Miyahara, 2008; Souteyrand et al., 1997). The inherent miniaturization of FET biosensors and their compatibility with microfabrication processes make them attractive for integration into microfluidic and micro-analytical devices. Moreover, the configuration of an extended gate structure facilitates modification of sensor chips in a cost-effective way. However, highly sensitive detection of weakly charged or uncharged analytes remained a major challenge (Goda and Miyahara, 2010b; Matsumoto et al., 2009). The use of structured oligonucleotide aptamer probes together with a groove binder or intercalating species extends the utility of the FET biosensor to detect a wide variety of target species independently of their intrinsic electric charges. The use of a DNA binder that is less carcinogenic and mutagenic than DAPI would improve the safety of the assay (Ferguson and Denny, 2007). Alternatively, preloading a therapeutic anticancer agent that is capable of binding to the stem of a hairpin aptamer probe (e.g., doxorubicin and cisplatin) might realize a stimuli-responsive release of the drug upon recognition of a specific biomarker for cancer or tumors. The aptamer FET biosensor has a potential for applications to theranostics, in which diagnostics and therapy are autonomously and simultaneously performed with the aid of "smart" molecules similar to the hairpin aptamer used in the study (Janib et al., 2010; McCarthy et al., 2006; Moon et al., 2011; Sanson et al., 2011; Sumer and Gao, 2008; Xie et al., 2010). An additional feature of the technology is that the signal induction by the release of a charged indicator from the electrical double layer at the gate-solution nano-interface may overcome the potential drawback of counterion-screening for charged analytes in FET biosensing. Our technique may allow large molecules with shielded intrinsic charges to be detected using a target-specific sh-aptamer combined with a cationic groove binder.

4. Conclusions

The sensitive and specific detection of ATP was achieved in label-free and temperature-dependent manners by monitoring the release of a cationic indicator from the sh-aptamer incorporated in a FET biosensor. The potentiometric signal was generated by dissociation of preloaded DAPI from the stem of the hairpin into the bulk solution caused by the target-induced self-denaturation and formation of an aptamer-ATP complex. The structured aptamer concept as a molecular switch allows detection of neutral adenosine as well as negatively charged ATP with minimal influence of the charge-screening in a buffer solution using the FET biosensors. The hairpin aptamer combined with FET functions as a smart molecular switch for transducing target recognition events into electronic signals.

Acknowledgments

This research was supported in part by JST-CREST. Preparation of gold electrodes was supported by the Nano-Integration Facility at the National Institute for Materials Science (NIMS).

Appendix A. Supplementary data

Supplementary data associated with this article can be found, in the online version, at doi:10.1016/j.bios.2011.12.022.

References

Banerjee, D., Pal, S.K., 2008. Journal of Physical Chemistry B 112 (3), 1016–1021.
Bergveld, P., 1986. Biosensors 2 (1), 15–33.
Bock, L., Griffin, L., Latham, J., Vermaas, E., Toole, J., 1992. Nature 355 (6360), 564–566.
Bonanni, A., Esplandiu, M.J., Pividori, M.I., Alegret, S., del Valle, M., 2006. Analytical and Bioanalytical Chemistry 385 (7), 1195–1201.
Bonanni, A., Pumera, M., 2011. Acs Nano 5 (3), 2356–2361.
Famulok, M., Hartig, J.S., Mayer, G., 2007. Chemical Reviews 107 (9), 3715–3743.
Ferguson, L.R., Denny, W.A., 2007. Mutation Research – Fundamental and Molecular Mechanisms of Mutagenesis 623 (1–2), 14–23.
Fritz, J., Cooper, E.B., Gaudet, S., Sorger, P.K., Manalis, S.R., 2002. Proceedings of the National Academy of Sciences of the United States of America 99 (22), 14142–14146.
Fromherz, P., Offenhäusser, A., Vetter, T., Weis, J., 1991. Science 252 (5010), 1290–1293.
Goda, T., Miyahara, Y., 2010a. Analytical Chemistry 82 (5), 1803–1810.
Goda, T., Miyahara, Y., 2010b. Analytical Chemistry 82 (21), 8946–8953.
Goda, T., Miyahara, Y., 2011. Biosensors & Bioelectronics 26 (9), 3949–3952.
Gong, H., Zhong, T.Y., Gao, L., Li, X.H., Bi, L.J., Kraatz, H.B., 2009. Analytical Chemistry 81 (20), 8639–8643.
Huizenga, D.E., Szostak, J.W., 1995. Biochemistry 34 (2), 656–665.
Janib, S.M., Moses, A.S., MacKay, J.A., 2010. Advanced Drug Delivery Reviews 62 (11), 1052–1063.
Jayasena, S., 1999. Clinical Chemistry 45 (9), 1628–1650.
Kajiyama, T., Miyahara, Y., Kricka, L.J., Wilding, P., Graves, D.J., Surrey, S., Fortina, P., 2003. Genome Research 13 (3), 467–475.
Lee, C.S., Kim, S.K., Kim, M., 2009. Sensors 9 (9), 7111–7131.
Li, W., Nie, Z., Xu, X.H., Shen, Q.P., Deng, C.Y., Chen, J.H., Yao, S.Z., 2009. Talanta 78 (3), 954–958.
Liu, J.W., Cao, Z.H., Lu, Y., 2009. Chemical Reviews 109 (5), 1948–1998.
Liu, X.G., Qu, X.J., Dong, J., Ai, S.Y., Han, R.X., 2011. Biosensors & Bioelectronics 26 (8), 3679–3682.
Livolant, F., Leforestier, A., 1996. Progress in Polymer Science 21 (6), 1115–1164.
Matsumoto, A., Sato, N., Sakata, T., Yoshida, R., Kataoka, K., Miyahara, Y., 2009. Advanced Materials 21 (43), 4372–4378.
McCarthy, J.R., Jaffer, F.A., Weissleder, R., 2006. Small 2 (8–9), 983–987.
Moon, G.D., Choi, S.-W., Cai, X., Li, W., Cho, E.C., Jeong, U., Wang, L.V., Xia, Y., 2011. Journal of the American Chemical Society 133 (13), 4762–4765.
Nutiu, R., Li, Y., 2003. Journal of the American Chemical Society 125 (16), 4771–4778.
Piatek, A., Tyagi, S., Pol, A., Telenti, A., Miller, L., Kramer, F., Alland, D., 1998. Nature Biotechnology 16 (4), 359–363.
Poghossian, A., Cherstvy, A., Ingebrandt, S., Offenhausser, A., Schoning, M.J., 2005. Sensors and Actuators B – Chemical 111, 470–480.
Poirier, G.E., Tarlov, M.J., 1994. Langmuir 10 (9), 2853–2856.
Privett, B.J., Shin, J.H., Schoenfisch, M.H., 2010. Analytical Chemistry 82 (12), 4723–4741.
Rentsch, S., Siegenthaler, H., Papastavrou, G., 2007. Langmuir 23 (17), 9083–9091.
Sakata, T., Miyahara, Y., 2008. Analytical Chemistry 80 (5), 1493–1496.
Sanson, C., Diou, O., Thevenot, J., Ibarboure, E., Soum, A., Brulet, A., Miraux, S., Thiaudiere, E., Tan, S., Brisson, A., Dupuis, V., Sandre, O., Lecommandoux, S., 2011. Acs Nano 5 (2), 1122–1140.
Souteyrand, E., Cloarec, J.P., Martin, J.R., Wilson, C., Lawrence, I., Mikkelsen, S., Lawrence, M.F., 1997. Journal of Physical Chemistry B 101 (15), 2980–2985.
Sriram, M., Vandermarel, G.A., Roelen, H., Vanboom, J.H., Wang, A.H.J., 1992. Biochemistry 31 (47), 11823–11834.
Steel, A.B., Herne, T.M., Tarlov, M.J., 1998. Analytical Chemistry 70 (22), 4670–4677.
Stern, E., Wagner, R., Sigworth, F.J., Breaker, R., Fahmy, T.M., Reed, M.A., 2007. Nano Letters 7 (11), 3405–3409.
Sumer, B., Gao, J., 2008. Nanomedicine 3 (2), 137–140.
Tang, Z., Mallikaratchy, P., Yang, R., Kim, Y., Zhu, Z., Wang, H., Tan, W., 2008. Journal of the American Chemical Society 130 (34), 11268–11269.
Tinland, B., Pluen, A., Sturm, J., Weill, G., 1997. Macromolecules 30 (19), 5763–5765.
Tyagi, S., Bratu, D., Kramer, F., 1998. Nature Biotechnology 16 (1), 49–53.
Tyagi, S., Kramer, F., 1996. Nature Biotechnology 14 (3), 303–308.
Urata, H., Nomura, K., Wada, S., Akagi, M., 2007. Biochemical and Biophysical Research Communications 360 (2), 459–463.
Van Hooijdonk, C.A., Glade, C.P., Van Erp, P.E., 1994. Cytometry 17 (2), 185–189.
Wang, Y.Y., Liu, B., 2008. Analyst 133 (11), 1593–1598.
Wilson, D., Szostak, J., 1999. Annual Review of Biochemistry, 611–647.
Xie, J., Lee, S., Chen, X., 2010. Advanced Drug Delivery Reviews 62 (11), 1064–1079.
Yang, D.F., Wilde, C.P., Morin, M., 1996. Langmuir 12 (26), 6570–6577.
Yao, W., Wang, L., Wang, H.Y., Zhang, X.L., Li, L., 2009. Biosensors & Bioelectronics 24 (11), 3269–3274.
Zhang, J.Q., Wang, Y.S., He, Y., Jiang, T., Yang, H.M., Tan, X., Kang, R.H., Yuan, Y.K., Shi, L.F., 2010. Analytical Biochemistry 397 (2), 212–217.
Zhen, S.J., Chen, L.Q., Xiao, S.J., Li, Y.F., Hu, P.P., Zhan, L., Peng, L., Song, E.Q., Huang, C.Z., 2010. Analytical Chemistry 82 (20), 8432–8437.